J. At. Mol. Sci.
doi: 10.4208/jams.032012.042812a

Vol. **4** , No. 2 , pp. 121-128
May 2013

Theoretical study of the stereo-dynamics of the reaction H+CH$\rightarrow$ H_2+C(^{1}D)

Xing Li*

State Key Laboratory of Molecular Reaction Dynamics, Dalian Institute of Chemical Physics, Chinese Academy of Science, Dalian 116023, China

Received 20 March 2012; Accepted (in revised version) 28 April 2012
Published Online 28 March 2013

Abstract. The vector correlations between products and reagents for the reactions H+CH$\rightarrow$ H_2+C(^{1}D) at different collision energy have been studied by using the quasi-classical trajectories (QCT) on an ab initio potential energy surface of 1A′ symmetry. Four polarization-dependent generalized differential cross-sections (PDDCSs) have been calculated in center-of-mass (CM) frame. The distribution $P(\theta_r)$ of the angle between k and j', the distribution $P(\phi_r)$ of dihedral angle denoting $k-k'-j'$ correlation in the form of polar plots are calculated as well. The effect of deep well in potential surface and differ collision energies on the alignment and the orientation of product molecule H_2 rotational angular momentum vectors j' is revealed.

PACS: 31.30.jc, 33.15.Mt

Key words: quasi-classical trajectories, vectors correlations, stereodynamics

1 Introduction

In the recent decade, the CH_2 reactive system have been received considerable attention because of their importance in combustion reactions[1], gasification of coal[2], and astrochemistry[3]. For instance, the generation of methylene radical CH_2 by the title reaction is a key parameter in the chemistry of hydrocarbon combustion. From a practical perspective, CH_2 reactive system has important implications in organic chemistry, particularly in understanding the mechanisms of a large number of carbon-alkane reactions. Much experiment have focused on the C(^{1}D)+ $H_2\rightarrow$ CH+H reaction[4-9]. In recent years, Bergeat *et al.* measured the product angular and time-of -flight (TOF) distribution for the C(1D)+ H_2 reaction using the crossed molecular beam (CMB) experiment[10]. Balucani *et al.* obtained the product angular and velocity distributions in crossed beam experiments[11].

*Corresponding author. *Email address:* xingli@dicp.ac.cn (X. Li)

Theoretically, CH_2 reactive system contains only eight electrons and is thus amenable to high level ab initio calculations of its potential energy surface. Indeed, a highly accurate global potential energy surface of the 1A'state has been reported by Bussery-Honvault *et al.*[12]. They constructed the PES of CH_2 system and calculated the reaction probabilities for the reaction $C(^1D)+ H_2$ and present that the state-to state reaction probabilities as a function of the collision energy show a dense resonance structure, which is the first time reported for this type of atom + diatom reaction. Subsequently, the availability of the high quality potential energy surface has stimulated several dynamical studies of the reaction $C(^1D)+H_2$. Balucani *et al.*[13] performed the quantum mechanical (QM) scattering calculations and quasi-classical trajectory (QCT) calculations for the translational energy distributions. Banares *et al.* calculated integral and differential cross sections at 80meV collision energy and they also obtained the total and vibrationally state-resolved reaction probabilities in the 0-0.5eV collision energy range. Later, wave packet studies for integral cross sections and rate constants were reported by Lin and Guo[14,15].

As mentioned above, most of the studies so far have focused on the $C(^1D)+H_2 \rightarrow CH+H$ reaction. Because the importance in atmospheric and combustion chemistry, we also should pay attention to the reverse reaction $H+CH \rightarrow H_2+C(^1D)$. However, we have not found any experimentally nor theoretically research about the reverse reaction. This work is the first example for reverse reaction $H+CH \rightarrow H_2+C(^1D)$. Although the QCT method yields important information with relatively low computational costs, the results may be plagued by the neglect of quantum effects such as zero-point energy and tunneling. These difficulties have until now prevented us from an accurate result of scalar properties, such as reaction probability, reactive cross sections, thermal rate coefficient. However, vector properties (such as velocities and angular momentum) based on QCT calculation will be more accurate. In order to understand the dynamics of the H+CH reaction completely, it is necessary to study its vector properties, which can provide more information about chemical reaction stereo-dynamics [16-30]. By comprehending the scalar and vector properties together, the full picture of the scattering dynamics can be presented.

2 Quasi-classical trajectory calculations

In this paper we only summarize the details relevant to the present work. In the center-of-mass (CM) frame shown in Fig. 1, the reagent relative velocity vector k is parallel to the z-axis. The $x-z$ plane is the scattering plane containing the initial and final relative velocity vectors, k and k'. θ_t is the angle between the reagent relative velocity and product relative velocity, namely, scattering angle. The angles θ_r and ϕ_r are the polar and azimuthal angles of the final rotational momentum j'. The distribution function $P(\theta_r)$ describing the $k-k'$ correlation can be expanded in a series of Legendre polynomials [24] and the dihedral angle distribution function $P(\phi_r)$ describing the $k-k'-j'$ correlation expanded in a Fourier series. The full three-dimensional angular distribution associated

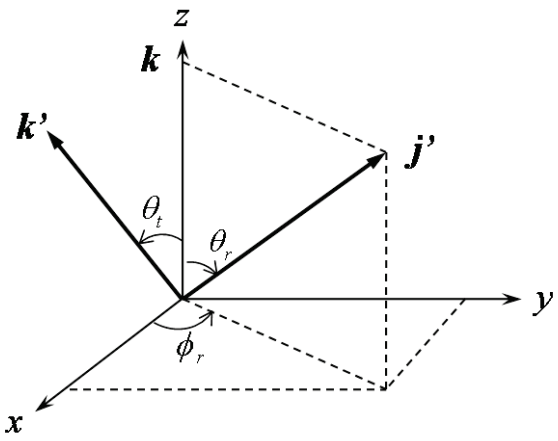

Figure 1: The center-of-mass coordinate system used to describe the k, k' and j' distribution.

with $k-k'-j'$ can be represented by a set of generalized polarization-dependent differential cross-sections (PDDCSs) in the CM frame that is described in Ref 22.

The calculations of product rotational polarization for the H+CH reaction have been performed on the BHL PES constructed by Bussery-Honvault *et al.*[12]. This potential energy surface has a calculated well depth of 99.7 kcal/mol relative to the C(^{1}D)+H_2 asymptote. The surface has no barrier for the perpendicular C_{2v} geometry, but presents a large barrier 12.35 kcal/mol for the collinear $C_{\infty v}$ geometry. The *ab initio* calculations were carried out over 1748 geometries and the resulting energies were fitted to a many body expansion.

The QCT calculations are standard [21, 25, 28] , which have been performed for the collision energies 0.3eV, 0,7eV and 1.1eV. The sixth-order symplectic routine with energy and total angular momentum conservations checked is used for the numerical solution[31]by running batches of 100,000 trajectories. The vibrational and rotational levels of the reactants molecules are taken as v=0 and j=0, respectively. The initial azimuthal orientation angle and polar angles for the reactant molecule internuclear axis is randomly sampled using Monte Carlo method.

3 Results and discussion

The polarization-dependent generalized differential cross-sections (PDDCSs) are the stereodynamical quantities amenable to direct experimental determination, in which they contain all the information about the $k-k'-j'$ vector correlation. The calculation of the PDDCSs for the title reaction on the BHL PES is shown in Fig. 3 with the corresponding collision energy of 0.3eV, 0.7eV and 1.1eV, respectively.

The PDDCS $[(2\pi/\sigma)(d_{00}/d_{\omega t})]$, which is simply proportional to the differential cross-section (DCS), only describes the $k-k'$ correlation or the scattering direction of the prod-

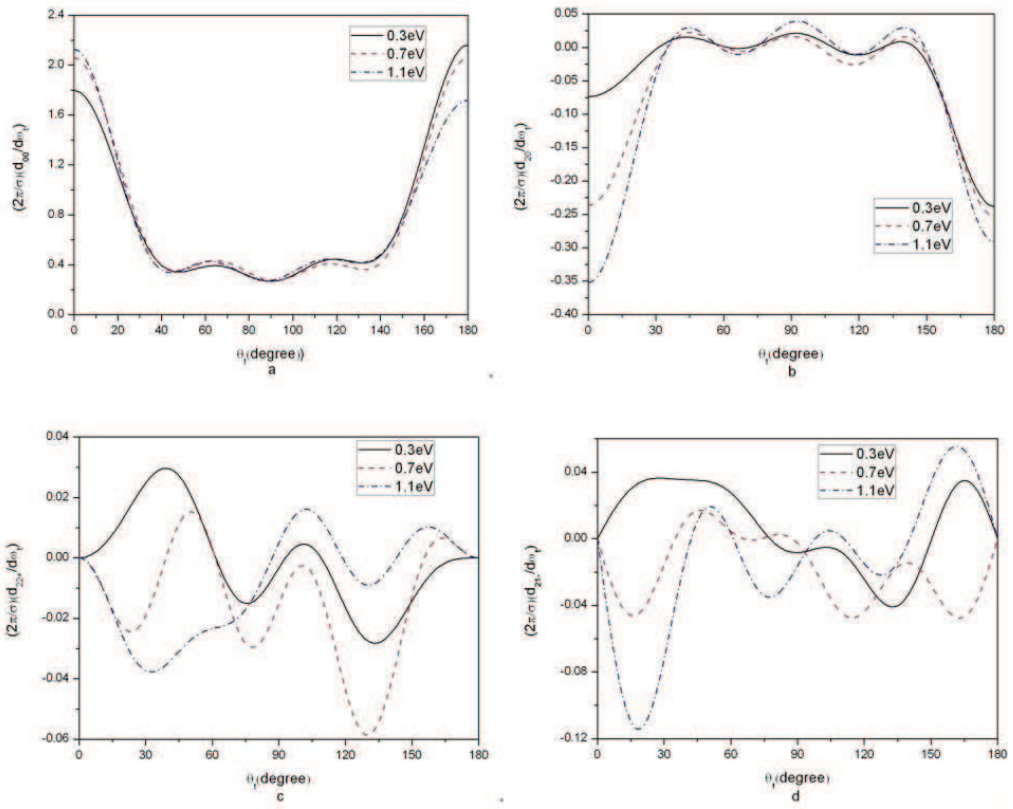

Figure 2: The polarization dependent generalized differential cross section of the title reaction for different collision energies. Panel (a) shows the PDDCS with $(k,q)=(0,0)$. Panels (b)-(d) depict the PDDCSs with $(k,q\pm)=(2,0)$, $(2,2+)$, and $(2,1-)$, respectively.

uct. As can be seen from Fig. 2(a), the products are both strongly scattered forward $(\theta_t = 0^\circ)$ and backward $(\theta_t = 180^\circ)$, and weakly symmetry for different collision energy. With the collision energy's increasing, the tendency of forward-scattering increases and the backward-scattering decreases. The PDDCS $[(2\pi/\sigma)(d_{20}/d_{\omega t})]$ is the expectation value of the second Legendre moment. As shown in Fig. 2(b), The behavior of $[(2\pi/\sigma)(d_{20}/d_{\omega t})]$ shows the trend is opposite to that of $[(2\pi/\sigma)(d_{00}/d_{\omega t})]$, which indicates that j' is aligned perpendicular to k. These result from the fact that the $[(2\pi/\sigma)(d_{20}/d_{\omega t})]$ is related to alignment moment $<P_2(\cos\theta_r)>$, and the calculated values of the $<P_2(\cos\theta_r)>$ are -0.327, -0.323 and -0.321 corresponding to the collision energy 0.3eV, 0.7eV and 1.1eV, respectively. Thus, the product rotational alignment at low collision energy is stronger than that at high collision energy.

It can be also seen in Fig. 2(c) and Fig. 2(d) that the PDDCSs with $q \neq 0$ are zero at the extremities of forward and backward scattering. The behavior of PDDCSs $q \neq 0$ at the scattering away from extreme forward and backward direction is more interesting. It

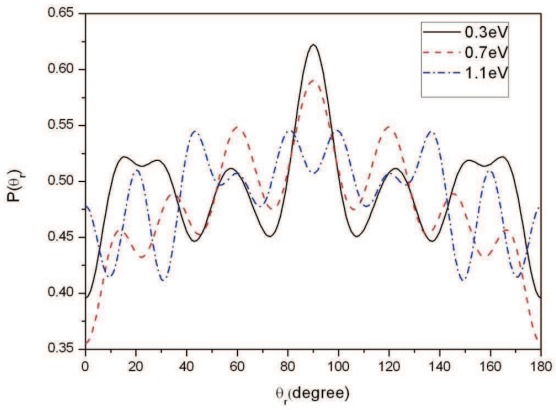

Figure 3: The distribution of $P(\theta_r)$, reflecting $k-j'$ correlation at different collision energies.

provides information on the ϕ_r dihedral angel distribution, and the fact that the values are nonzero at scattering angles away from $\theta_t = 0^\circ$ and 180° indicates that the $P(\theta_r,\phi_r)$ distribution is not isotropic for backward scattering products. The negative value of $[(2\pi/\sigma)(d_{22}+/d_{\omega t})]$, which is related to $<\sin 2\theta_r \cos 2\varphi_r>$, indicates the product alignment along the y-axis, while the positive value indicates the product alignment along the x-axis. Moreover, the larger the absolute value, the stronger the degree of product aligning along the corresponding axis. In Fig. 2(c), it can be seen that the value of $[(2\pi/\sigma)(d_{22}+/d_{\omega t})]$ is always negative around at $\theta_t = 130^\circ$, which indicate that the product is preferentially aligned along the y-axis at the scattering angle is around 130°. With the collision energy increase, the value of $[(2\pi/\sigma)(d_{22}+/d_{\omega t})]$ change from positive to negative at about 40°, the product alignment change from along x-axis to y-axis. At the scattering angle is about 100°, the product is aligned along the y-axis only on the collision energy 0.7eV. The value of $[(2\pi/\sigma)(d_{21}-/d_{\omega t})]$ is related to $<-\sin 2\theta_r \cos\varphi_r>$, and the behavior of it is similar to that of $[(2\pi/\sigma)(d-22+/d_{\omega t})]$. It is necessary to notice that the stronger polarization of the H2 for these three collision energies is all at about 15° and 165°. When the collision energy is 1.1eV, the value of $[(2\pi/\sigma)(d_{21}-/d_{\omega t})]$ is clearly positive at about 15, indicating the product alignment along the direction of vector x+z. It is interesting that, only at the collision energy is 0.7eV, the value of $[(2\pi/\sigma)(d_{21}-/d_{\omega t})]$ is negative at the scattering angle is about 165° and the product alignment along the direction of vector x-z. However, the collision energy is become larger or smaller, the direction will be along x+z.

To get a better graphical representation of the polarization of the product, the $P(\theta_r)$ and $P(\phi_r)$ distribution at different collision energy are shown in Fig. 3 and Fig. 4. The $P(\theta_r)$ distribution, as shown in Fig. 3, describes the $k-j'$ correlation. For three collision energies, the peaks of $P(\theta_r)$ are at θ_r=90° and symmetric with respect to 90°, which shows that j' is symmetry distributed in the product scattering frame and is always perpendicular to k. But the span of curves is broad, which shows that the product rotational angular

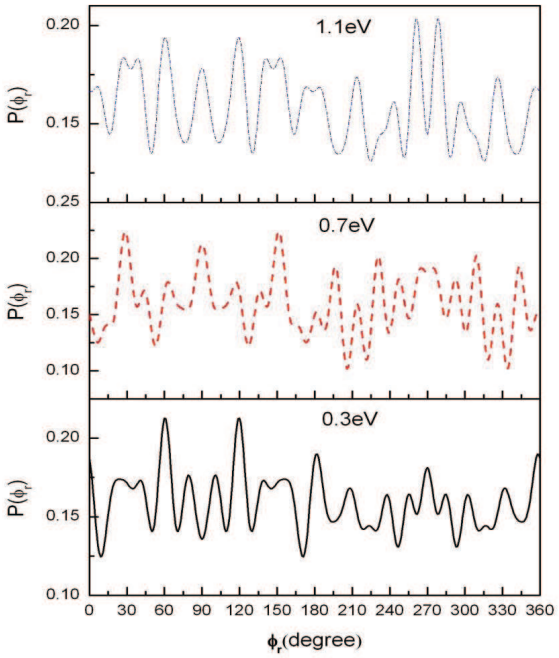

Figure 4: The dihedral angle distribution of $P(\phi_r)$, reflecting $k-k'-j'$ correlation at different collision energies.

momentum vector is weakly aligned along the direction at right angle to the relative velocity direction. It is also clear that the peak of $P(\theta_r)$ at θ_r closed to 90° is higher with the decrease of collision energy, indicating that the degree of alignment of production at low collision energy is slightly stronger. The reason for the results may be ascribed to the structure of the BHL PES which there is a deep well in the reaction path. Since the reaction rapidly strides over the well when the collision energy increases, there is no enough time for the molecule to rotate towards the preferred alignment direction. As a result, the product rotational angular momentum is weakly aligned at high collision energy. The dihedral angle distribution $P(\phi_r)$ shown in Fig. 4 describe $k-k'-j'$ correlations. These $P(\phi_r)$ distributions tend to be asymmetric with respect to the $k-k'$ scattering plane, directly reflecting the strong polarization of product rotational angular momentum. As seen in Fig. 4, there is no obvious single peak of $P(\phi_r)$ for the three different collision energy. This means that the product rotational angular momentum vector j' is no preferentially alignment and orientation. The reason for the results is the existence of the deep well in the PES and the participation of long-lived resonance states during the reaction process.

It seems interesting that the title reaction is symmetric about the relative velocity vector, while the distribution of $P(\phi_r)$ is asymmetric. For the reaction $H+C(^1D)H \rightarrow H_2+C(^1D)$ orientation of the product H_2 results from the repulsive energy between H and C atoms, which leads to the violation of the symmetry when the reaction occurs.

According to the impulse model[28, 32] about the molecular reaction for the reaction $A+BC\rightarrow AB+C$, we have

$$j'=L\sin^2\beta+j\cos^2\beta+J_1m_B/m_{AB},$$

where L is the reagent orbital angular momentum and $J_1=\sqrt{\mu_{BC}}(r_{AB}\times r_{CB})$, r_{AB}, r_{CB} are unit vectors, where B points to A and C, respectively; μ_{BC} is the reduced mass of the BC molecule and R is the repulsive energy. During the chemical-bond forming and breaking for reaction, the term $L\sin^2\beta+j\cos^2\beta$ in the equation is symmetric, while the term J_1m_B/m_{AB} shows a preferential direction because of the effect of repulsive energy, which leads to the orientation of the product H_2.

4 Conclusions

Quasi-classical trajectory calculations of the product rotational polarization for the reaction $H+CH\rightarrow H_2+C(^1D)(v=0,j=0)$ have been performed on BHL PES constructed by Bussery-Honvault *et al.* at different collision energies. The Four PDDCS predicts that the products H_2 mainly tends to closely backward-forward symmetric, and with the collision energy's increasing, the tendency of forward scattering increases to some extent. We get the $P(\theta_r)$ and $P(\phi_r)$ distribution at the different collision energy, Due to the deep well in the PES, the alignment and orientation for the product rotational angular momentum vectors are weak.

References

[1] A. G. Gaydon, The Spectroscopy of Flames (Chapman and Hall, London, 1974).
[2] A.Williams, M. Pourkashanian, and N. Skorupska, Combustion and Gasification of Coal(Taylor and Francis, New York, 2000).
[3] D. R. Flower and G. P. des Forets, Mon. Not. R. Astr. Soc. 297 (1998) 1182.
[4] D. Husain and L. J. Kirsch, Chem. Phys. Lett. 9 (1971) 412.
[5] G. M. Jursich and J. R. Wiesenfeld, Chem. Phys. Lett. 110 (1984) 14.
[6] G. M. Jursich and J. R. Wiesenfeld, J. Chem. Phys. 83 (1985) 910.
[7] K. Mikulecky and K. H. Gericke, Chem. Phys. 175 (1993) 13.
[8] K. Mikulecky and K. H. Gericke, J. Chem.Phys. 98 (1993) 1244.
[9] K. Sato, N. Ishida, T. Kurakata, A. Iwasaki, and S. Tsunashima, Chem. Phys. 237 (1998) 195.
[10] A. Bergeat, L. Cartechini, N. Balucani, G. Capozza, L. F. Phillips, P. Casavecchia, G. G. Volpi, L. Bonnet, and J. C. Rayez, Chem. Phys.Lett. 327 (2000) 197.
[11] N. Balucani, G. Capozza, E. Segoloni, A. Russo, R. Bobbenkamp, P. Casavecchia, T. Gonzalez-Lezana, E. J. Rackham, L. Banares, and F. J. Aoiz, J. Chem. Phys. 122 (2005) 234309.
[12] B. Bussery-Honvault, P. Honvault, and J. M. Launay, J.Chem. Phys. 115 (2001) 10701.
[13] N. Balucani, G. Capozza, L. Cartechini, A. Bergeat, R. Bobbenkamp, P. Casavecchia, F. J. Aoiz, L. Banares, P. Honvault, B. Bussery-Honvault, and J. M. Launay, Phys. Chem. Chem. Phys. 6 (2004) 4957.
[14] S. Y. Lin and H. Guo, J. Phys. Chem. A 108 (2004) 10066.

[15] S. Y. Lin and H. Guo, J. Chem. Phys. 119 (2003) 11602.
[16] Y. F. Liu, Y. Wang, and Z. L. Zhu, J. At. Mol. Phys. 19 (2002) 19 (in Chinese).
[17] J. F. He and P. Z. Ding, J. At. Mol. Phys. 24 (2007) 132 (in Chinese).
[18] Y. F. Liu, H. Y. Meng, and S. L. Cong, J. At. Mol. Phys. 22 (2005) 119 (in Chinese).
[19] D. A. Case, G. M. McClelland, and D. R. Herschbach, Mol. Phys. 35 (1978) 541.
[20] S. K. Kim and D. R. Herschbach, Fara. Dis. 84 (1987) 159.
[21] K. L. Han, L. Zhang, D. L. Xu, G. Z. He, and N. Q. Lou, J. Phys. Chem. A 105 (2001) 2956.
[22] L. P. Ju, K. L. Han, and J. Z. H. Zhang, J. Comput. Chem. 30(2009)305.
[23] K. L. Han, G. Z. He, and N. Q. Lou, J. Chem. Phys. 105 (1996) 8699.
[24] A. J. Orrewing and R. N. Zare, Annu. Rev. Phys. Chem. 45 (1994) 315.
[25] M. L. Wang, K. L. Han, and G. Z. He, J. Chem. Phys. 109 (1998) 5446.
[26] M. L. Wang, K. L. Han, and G. Z. He, J. Phys.Chem. A 102 (1998) 10204.
[27] M. D. Chen, K. L. Han, and N. Q. Lou, J. Chem. Phys. 118 (2003) 4463.
[28] M. D. Chen, K. L. Han, and N. Q. Lou, Chem. Phys. Lett. 357 (2002) 483.
[29] Q. Wei, X. Li, and T. Li, Chem. Phys. 368 (2010) 58.
[30] Q. Wei, X. Li, and T. Li, Chinese J. Chem. Phys. 22 (2009) 523.
[31] X. Zhang and K. L. Han, Int. J. Quan. Chem. 106 (2006) 1815.
[32] R. J. Li, K. L. Han, F. E. Li, R. C. Lu, G. Z. He, and N. Q. Lou, Chem. Phys. Lett. 220 (1994) 281.